

Evaluation of the CLM4 Lake Model at a Large and Shallow Freshwater Lake*

BIN DENG

*Yale–NUIST Center on Atmospheric Environment, Nanjing University of Information, Science and Technology, Nanjing, China,
and School of Forestry and Environmental Studies, Yale University, New Haven, Connecticut*

SHOUDONG LIU, WEI XIAO, AND WEI WANG

Yale–NUIST Center on Atmospheric Environment, Nanjing University of Information, Science and Technology, Nanjing, China

JIMING JIN

Department of Watershed Sciences, Utah State University, Logan, Utah

XUHUI LEE

*Yale–NUIST Center on Atmospheric Environment, Nanjing University of Information, Science and Technology, Nanjing, China,
and School of Forestry and Environmental Studies, Yale University, New Haven, Connecticut*

(Manuscript received 10 May 2012, in final form 15 November 2012)

ABSTRACT

Models of lake physical processes provide the lower flux boundary conditions for numerical predictions of weather and climate in lake basins. So far, there have been few studies on evaluating lake model performance at the diurnal time scale and against flux observations. The goal of this paper is to evaluate the National Center for Atmospheric Research Community Land Model version 4–Lake, Ice, Snow and Sediment Simulator using the eddy covariance and water temperature data obtained at a subtropical freshwater lake, Lake Taihu, in China. Both observations and model simulations reveal that convective overturning was commonplace at night and timed when water switched from being statically stable to being unstable. By reducing the water thermal diffusivity to 2% of the value calculated with the Henderson–Sellers parameterization, the model was able to reproduce the observed diurnal variations in water surface temperature and in sensible and latent heat fluxes. The small diffusivity suggests that the drag force of the sediment layer in this large (2500 km²) and shallow (2-m depth) lake may be strong, preventing unresolved vertical motions and suppressing wind-induced turbulence. Model results show that a large fraction of the incoming solar radiation energy was stored in the water during the daytime, and the stored energy was diffused upward at night to sustain sensible and latent heat fluxes to the atmosphere. Such a lake–atmosphere energy exchange modulated the local climate at the daily scale in this shallow lake, which is not seen in deep lakes where dominant lake–atmosphere interactions often occur at the seasonal scale.

1. Introduction

Lakes and other inland water bodies occupy approximately 4.6×10^6 km², or 4%, of the land surface of the

earth (Downing et al. 2006). Owing to their high heat capacity and low albedo, lakes as heat buffers have significant impacts on local and regional weather and climate (Hostetler et al. 1994; Bonan 1995; Lofgren 1997; Krinner 2003; Long et al. 2007; Samuelsson et al. 2010; Subin et al. 2012a). During early winter and late spring, storm formations are frequently enhanced in the areas downwind of midlatitude lakes under conditions of high surface evaporation and strong air instability (Zhao et al. 2012). Lakes are aerodynamically much smoother than land surfaces; this water–land discontinuity contributes to variations of the atmospheric flow over the landscape

* Supplemental information related to this paper is available at the Journals Online website: <http://dx.doi.org/10.1175/JHM-D-12-067.s1>.

Corresponding author address: Xuhui Lee, School of Forestry and Environmental Studies, Yale University, 195 Prospect St., New Haven, CT 06511.
E-mail: xuhui.lee@yale.edu

(Samuelsson and Tjernström 2001; Törnblom et al. 2007). In addition, lakes play an important role in the global carbon cycle, acting as sources of greenhouse gases through biogeochemical processes of carbon redistribution and mineralization (Cole et al. 2007; Battin et al. 2009; Downing et al. 2008; Tranvik et al. 2009).

Predictions of weather and climate in lake basins rely on lake models for surface heat, water, and momentum fluxes as the lower boundary conditions. In these models, the lake surface temperature is solved from the surface energy balance equation, and the fluxes of momentum and sensible and latent heat are calculated with bulk formulations (e.g., Oleson et al. 2004). Generally, these models assume that the horizontal gradients of temperature and salinity are substantially smaller than their vertical counterparts; thus, the state and flux variables are typically resolved only in the vertical direction. With respect to the parameterization of vertical mixing, a critical process affecting the redistribution of energy in the lake and between the lake and atmosphere aloft, lake models typically fall into two categories: the eddy diffusion type (e.g., Hostetler et al. 1994; Fang and Stefan 1998; Oleson et al. 2004; Subin et al. 2012b) and the turbulence-based type (e.g., Imberger et al. 1978; Goudsmit et al. 2002; Stepanenko and Lykosov 2005). The eddy diffusion type models consist of a prognostic equation for lake temperature in which vertical mixing is contributed by molecular and eddy diffusion, with the latter being two to three orders of magnitude larger than the former (e.g., Oleson et al. 2004). For eddy diffusivity, Henderson-Sellers (1985) proposed a parameterization based on surface wind speed and lake stratification. Despite the lack of a comprehensive evaluation against experimental data, the parameterization of Henderson-Sellers has been widely adopted in the eddy-diffusion-type models. In comparison, the turbulent-based type of models, also known as k - ϵ models, relate the eddy diffusivity to the turbulent kinetic energy (TKE or k) and its dissipation rate (ϵ) according to the Kolmogorov-Prandtl relation (e.g., Burchard and Baumert 1995), requiring two additional prognostic equations for k and ϵ . These two types of models have been widely used in studies of lake-atmosphere interactions, albeit their tendency to break down in the hypolimnion where the temperature gradient is often weak (MacKay et al. 2009). In addition to these two types of models, Mironov (2008) proposed the Freshwater Lake model (FLake), which assumes self-similarity for the temperature-depth profile in the stratified layer as well as integral budgets of the mixed layer above and the bottom layer below. In FLake, eddy diffusivity is parameterized as a function of eddy length scale and TKE.

Like any other land surface schemes, offline evaluation of lake models against field observations is an important

step before they are used for weather and climate predictions. Most of the evaluation studies have been performed at individual lakes (Hostetler and Bartlein 1990; Boyce et al. 1993; Peeters et al. 2002; Perroud et al. 2009; Voros et al. 2010). Recently, a more comprehensive evaluation, the Lake Model Intercomparison Project (LakeMIP), was carried out with the aim to compare eight one-dimensional lake models against observations, focusing, in the first phase, on temperate and boreal lakes (Stepanenko et al. 2010). For weather and climate studies, it is the performance of model-predicted surface fluxes that matters most because the planetary boundary layer (PBL) scheme is driven by these fluxes. So far, these evaluation studies have been restricted to comparison against observed seasonal and annual cycles of water temperature, with only a few exceptions that provide additional evaluation of model-predicted surface fluxes against indirect flux estimates (Hostetler and Bartlein 1990; Stepanenko et al. 2010; Martynov et al. 2010; Subin et al. 2012b). Indirect flux estimates are obtained using the mass transfer (e.g., Laird and Kristovich 2002) or the surface energy budget method (e.g., Lenters et al. 2005) and are subject to uncertainties in the parameters used and in how the energy flux components are partitioned. In comparison, direct field measurements using the eddy-covariance (EC) method are considered to provide more accurate and reliable flux data for model validation for dry-land ecosystems (e.g., Wood et al. 1998). However, because of logistical difficulty, in situ EC measurements on lakes, especially over seasonal and annual cycles, have been rare, except in recent years (e.g., Blanken et al. 2000; Vesala et al. 2006; Rouse et al. 2008; Liu et al. 2009; Blanken et al. 2011; Nordbo et al. 2011). To date, we are not aware of studies that evaluate lake model-predicted surface fluxes against in situ EC observations.

In this study, we aim at evaluating the Community Land Model version 4-Lake, Ice, Snow and Sediment Simulator (CLM4-LISSS) (Subin et al. 2012b) at Lake Taihu in Jiangsu Province, China—a shallow (2 m deep) and large ($\sim 2500 \text{ km}^2$) freshwater lake where EC measurements of surface fluxes are available. CLM4-LISSS is an improved version of the lake model embedded in CLM4 (Oleson et al. 2004) and is well suited for a wide spectrum of weather and climate studies (Subin et al. 2012a). Our goal is threefold: 1) to quantify the sensitivity of the model performance to various intrinsic and external model parameters, 2) to evaluate the model-predicted fluxes of sensible and latent heat against the observed fluxes, and 3) to investigate the time evolution of the energy flux partitioning in response to solar radiation forcing. Our work complements the study by Subin et al. (2012a,b). In their study, CLM4-LISSS is optimized for

application in global climate models, and its performance is evaluated at seasonal to multiyear time scales. The present study seeks to optimize the model parameter values at the diurnal time scale. This scale is relevant to local phenomena such as PBL growth, lake breeze circulations, and mixing of chemical constituents in the water. Although the study is restricted to CLM4-LISSS, the physical insights gained can be extended to other types of lake models.

Lake Taihu is chosen for three reasons. First, we are not aware of a detailed model evaluation study for a subtropical lake. When compared with other lakes in middle to high latitudes, Lake Taihu does not generate strong lake effect storms or lake–land breeze circulations. Second, a research emphasis in the past has been on evaluating modeled thermal structures in deep lakes (e.g., Lofgren 1997; Long et al. 2007). This emphasis is justified on the ground that lake processes are much more difficult to simulate than those of shallow lakes. Still, shallow lakes deserve attention because mixing regimes in these lakes tend to vary at finer time scales than in deep lakes. Third, the catchment of Lake Taihu represents only 0.4% of China's land area but contributes nearly 12% of the national gross domestic product (An and Wang 2008). The intensive economic activities have created severe pollution stress on the lake system (e.g., Wang et al. 2011). A validated lake model may be a useful tool to aid the ongoing lake restoration efforts, such as for the calculations of lake water temperature for the prediction of algal outbreaks.

2. Methods

a. Site and data

The main experiment was conducted in Meiliangwan (MLW) Bay, which is situated in the north part of Lake Taihu (31°24'N, 120°13'E; Fig. 1). An eddy covariance system, consisting of a three-dimensional sonic anemometer/thermometer (model CSAT3, Campbell Scientific Inc., Logan, Utah, United States) and an open-path infrared gas analyzer (model LI7500, Li-Cor Inc., Lincoln, Nebraska, United States), was employed to measure the three-dimensional wind speed, air temperature, and atmospheric H₂O and CO₂ concentrations at 10 Hz. Fluxes of momentum (τ), sensible heat (Q_H), and latent heat (Q_E) were computed from the 10-Hz time series over 30-min intervals. The measurement was at 3.5 m above the water surface and approximately 150 m away from the shore. A net radiometer (model CNR4, Kipp & Zonen B.V., Delft, the Netherlands) was used to measure the four components of the surface radiation balance (incoming shortwave, reflected shortwave,

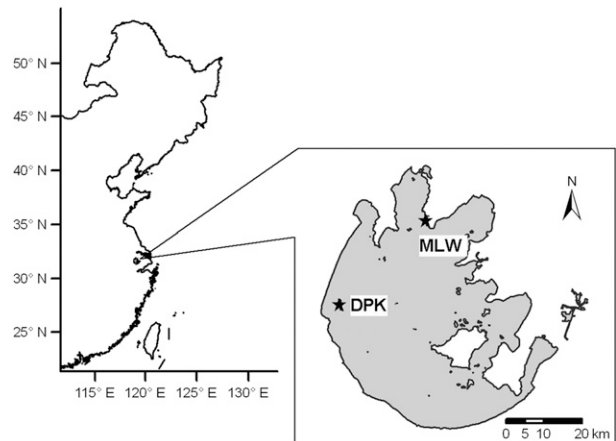


FIG. 1. Map showing the location of Lake Taihu and the two measurement sites.

incoming longwave, and outgoing longwave radiation). A standard micrometeorology system (model Dynamet, Dynamax Inc., Houston, Texas, United States) was used to measure air temperature, relative humidity, and wind speed and direction at a height 4.0 m above the water surface. Water temperature at 20-cm, 50-cm, 100-cm, and 150-cm depths and temperature of the lake sediment were measured using temperature probes (model 109-L, Campbell Scientific Inc.). The temperature of the water surface was calculated from the outgoing longwave radiation using the Stefan–Boltzmann law. In this study, we used the data collected from 13 June [day of year (DOY) 164] 2010 to 2 July (DOY 183) 2011. The complete dataset used for the model calibration and validation is available as an online supplement to this paper (<http://dx.doi.org/10.1175/JHM-D-12-067.s1>) and also at http://pantheon.yale.edu/~xhlee/online_data_supplement_deng.zip.

A second measurement platform, the Dapuko (DPK) site (Fig. 1), is located on the west side of the lake. DPK is about 2 km from the shore and 30 km linear distance away from MLW. The measured variables included the four radiation components, wind speed, air temperature, and humidity. This site was much windier than MLW, with wind speed typically 100% greater than that at MLW. The annual mean air temperature at Lake Taihu is 16.3°C, and annual precipitation is 1360 mm. The lake is ice free throughout the year.

b. CLM4-LISSS and its calibrated version

CLM4-LISSS is an improved version of CLM4-Lake, developed by scientists at the National Center of Atmospheric Research and the Lawrence Berkeley National Laboratory (Oleson et al. 2004; Subin et al. 2012a,b). The core structure of the model can be traced to Hostetler

et al. (1993, 1994), Bonan (1995), and Zeng et al. (2002). It consists of three component modules: namely, a surface module for flux estimation, a lake module for updating lake temperature, and a hydrology module for updating hydrological components. CLM4-LISSS is improved over CLM4-Lake by adopting more accurate representations of lake processes. For example, CLM4-LISSS takes into account the enhanced diffusion due to unresolved 3D processes and, thus, significantly improves the flux simulations for deep lakes. It is unclear, however, if the same enhancement is required for shallow lakes.

The eddy diffusivity k_e parameterization is that of Henderson-Sellers (1985). It does not explicitly resolve the interfacial skin layer of the water surface. In this layer, molecular processes play an important role in heat diffusion. There is observational evidence that the temperature of this layer can be quite different from that of the deeper water (Oesch et al. 2005; Frew et al. 2004).

To compute the lake surface temperature, CLM4-Lake and CLM4-LISSS make use of the energy balance equation of the lake surface layer:

$$\beta K^* + (L_{\downarrow} - L_{\uparrow}) = Q_H + Q_E + Q_g, \quad (1)$$

where K^* is net shortwave radiation; β is the fraction of K^* retained in the lake surface layer; L_{\downarrow} and L_{\uparrow} are incoming and outgoing longwave radiation, respectively; Q_H is sensible heat flux; Q_E is latent heat flux; and Q_g is the diffusion heat flux between the lake surface layer and the rest of the lake. The lake surface temperature is solved from this equation at every time step of integration. In CLM4-Lake, β in Eq. (1) is erroneously set to unity. This error introduces additional energy into the lake system and leads to overestimation of the lake surface temperature (T_s). The error has now been fixed in CLM4-LISSS, and β is allowed to vary.

For dry-land ecosystems, the energy balance equation is often expressed at the land surface. The energy balance of the *lake surface* is given by

$$K^* + (L_{\downarrow} - L_{\uparrow}) = Q_H + Q_E + Q_g + (1 - \beta)K^*. \quad (2)$$

In this equation, $Q_g + (1 - \beta)K^*$ is the heat storage term whose effect is to raise the water temperature if it is positive and reduce the water temperature if it is negative. Unlike dry-land ecosystems, whose heat storage in the soil is caused only by heat diffusion, here the storage term is contributed by both heat diffusion and transmission of solar radiation in the water column, the latter of which follows the description of Beer's law.

Once the lake surface temperature is known, the surface fluxes Q_H and Q_E are calculated using the bulk approach, where the flux is proportional to the difference

in temperature or specific humidity between lake surface and the reference height, with the proportionality coefficient dependent on wind speed and thermal roughness (Oleson et al. 2004). The diffusion of heat between the water layers follows the heat diffusion equation, whose diffusivity k_e is parameterized as a function of the momentum flux at the surface and thermal stratification in the water.

c. Setup of model simulations

The model was forced by hourly air temperature, humidity, and wind speed observed at a height of 4.0 m above the water surface. Additional forcing variables were net shortwave radiation K^* and incoming longwave radiation L_{\downarrow} . The vertical grid spacing was 0.2 m, and the time step of integration was 30 min. A spinup time of one year was used to remove the effect of the initial conditions and to bring the sediment layer into thermal equilibrium with the overlying water. Model tests revealed that the simulated surface temperature became insensitive to the initial conditions after 10 days of integration.

There are two groups of model parameters, external and internal. The external parameters are site specific, including lake depth (2.0 m in this study) and light extinction coefficient η . In the original CLM4-LISSS, from the lake surface down to the depth of 0.6 m, the near-infrared radiation is absorbed while the visible radiation penetrates. Therefore, β is approximated as the near-infrared fraction, which can be calculated as a function of atmospheric conditions and solar zenith angle. This specification is not suitable for this study because we had to use a small vertical grid spacing and, as such, some infrared radiation was able to penetrate through the surface layer. Furthermore, when containment is present, the absorption difference is significantly reduced between the visible and the infrared bands (Pegau et al. 1997; Huang et al. 2009). In our offline test, β was prescribed. Instead of setting β to a constant, such as 0.4 as commonly used in the literature (Oleson et al. 2004), we related β to η according to Beer's law such that the energy balance was conserved in vertical:

$$\beta = 1 - e^{-z_a \eta}, \quad (3)$$

where z_a is the thickness of the surface water layer. Equation (3) describes the penetration of the shortwave (visible and infrared) radiation and implies that the larger the η , or the dirtier the water, the more solar radiation will be retained in the surface layer. This relationship allows us to examine the transient response of the lake energy balance to changes in water quality. We set z_a to be 0.2 m; this small value is necessary considering that the lake is shallow and turbid. Huang et al.

(2009) made a profile observation of solar radiation at eight water depths at MLW. The best fit to their data with an exponential function yielded a value between 4 and 8 for η or 0.55–0.80 for β . In this study, η was set to 5 m^{-1} , unless stated otherwise.

The internal parameters describe the intrinsic physical properties of the energy and momentum exchange processes. In CLM4-LISSS, the momentum roughness length (z_{0m}) is a function of friction velocity, and the thermal (z_{0h}) and water vapor (z_{0q}) roughness length are parameterized as a function of z_{0m} . In this study, we set these parameters to constants ($z_{0m} = 3.3 \times 10^{-4} \text{ m}$; $z_{0h} = 1.9 \times 10^{-6} \text{ m}$; $z_{0q} = 3.9 \times 10^{-8} \text{ m}$). With these values, the bulk flux parameterizations provided the best fit to the observed eddy-covariance fluxes at MLW. They are also in excellent agreement with the roughness values inferred from other lake flux observations (Heikinheimo et al. 1999; Blanken et al. 2003; Liu et al. 2009; Nordbo et al. 2011). The eddy diffusivity (k_e) is driven by surface wind and modified by stable stratification and convective overturning. Heat diffusion in the underlying soil layer is calculated with a thermal conductivity prescribed for saturated soils. At both MLW and DPK, the sediment consists of a 1–2-m lacustrine stratum (muddy clay and sludge) and an underlying hard loess stratum (Shen et al. 2011). The surface albedo parameterization was not used because the net shortwave radiation (incoming minus reflected shortwave) flux was given as a forcing variable. Also not used were parameterizations of snow and ice processes as the lake remains ice-free throughout the year.

3. Results and discussion

a. Parameter sensitivity

Unlike deep lakes where turnover occurs at the seasonal time scale, Lake Taihu experienced turnover at the diurnal scale as a result of its shallowness (Fig. 2a). During daytime, the upper part of the lake absorbed more solar radiation and was thus warmer than the lower part, resulting in stable stratification that limited the wind-induced vertical mixing (Fig. 3a). During our study period, water temperatures were mostly greater than 4°C , so the warmer upper layer has lower water density and is therefore associated with a stable water column. The stable stratification was eroded quickly when the lake surface cooled down after sunset. The lake thus turned into a neutral or slightly unstable condition during nighttime.

The diurnal range of the surface temperature (T_s) was roughly 3.5°C for the period shown in Fig. 2a and was typical of Lake Taihu during the warm season. In

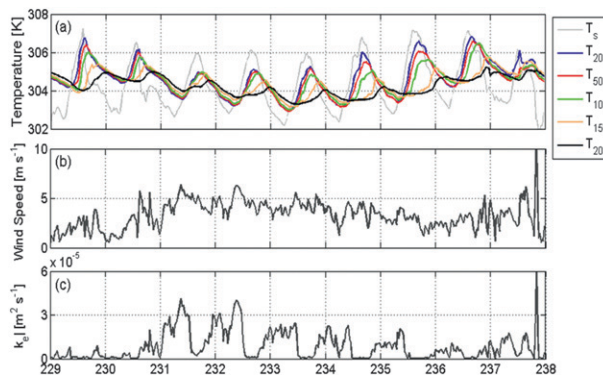


FIG. 2. Time series for DOY 229–238 (2010) at the MLW site: (a) water temperature measurements [the number in the subscript denotes the measurement depth (cm)], (b) surface wind speed measured at 3.5 m above the water, and (c) depth-averaged (0–2 m) eddy diffusivity calculated as 2% of the value based on the parameterization of Henderson-Sellers (1985).

comparison, the diurnal range at Sparkling Lake, Wisconsin, is much smaller ($\sim 0.8^\circ\text{C}$) (Martynov et al. 2010). The large diurnal range at Lake Taihu was caused in part by the high water turbidity, as noted above. Additionally, unlike almost all published studies where T_s is approximated with water temperature at a shallow depth (0.2–1 m), here T_s was measured with a pyrgeometer; use of water temperature at the 0.2-m depth would underestimate the diurnal variation in T_s by about 1°C (Fig. 2a).

As shown in Fig. 3b, CLM4-LISSS with the default k_e was not able to reproduce the observed stratification. Instead, the predicted lake temperature appears fairly uniform in the vertical. The corresponding T_s displays a diurnal variation noticeably smaller than that of the observations (Fig. 3d). Both features imply that the default k_e was too large for the lake, eroding stratification much more quickly than the observed value. We conclude that k_e should be adjusted to a smaller magnitude for a better estimation of T_s . A series of calculations were performed with k_e scaled down by a constant γ . It was found that a value of 2% for γ yielded good predictions of T_s (Fig. 3d) and reproduced some of the observed temperature stratifications (Fig. 3c).

Our result regarding k_e is in sharp contrast with many other studies in the literature. The k_e parameterization by Henderson-Sellers (1985), as adopted by CLM4-LISSS and other eddy-diffusion-type lake models, produced approximately the right amount of mixing for small lakes of shallow and medium depth. For deep lakes an upward adjustment by a factor of 10–100 is needed to produce correct seasonal variations in T_s and in thermal stratification (Martynov et al. 2010; Subin et al. 2012b), possibly because of mixing contributed by

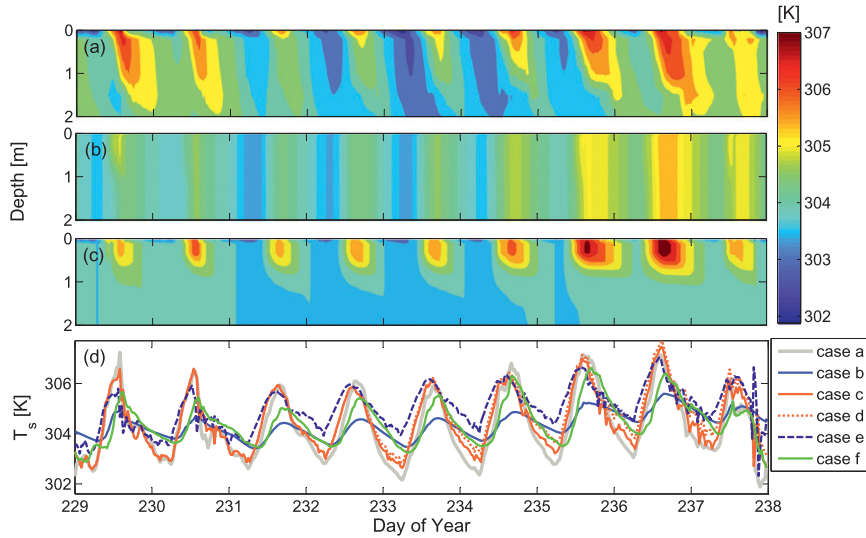


FIG. 3. Temperature comparison for DOY 229–238 (2010): contour plot of (a) observed temperature, (b) predicted temperature with default k_e , (c) predicted temperature with tuned k_e . (d) Surface temperature comparison for five scenarios: (case a) observation, (case b) prediction with default parameters, (case c) prediction with tuned k_e (using the surface temperature as the target variable for model optimization), (case d) similar to case b but for a step change of η from 5 to 1.4 m^{-1} at DOY 232, (case e) prediction with tuned k_e and original roughness lengths, and (case f) simulation using water temperature measurement at a 20-cm depth for model optimization.

3D circulations (Desai et al. 2009) that are unresolved by this 1D parameterization. To our knowledge, this study is the first one reporting large overestimation of the Henderson–Sellers parameterization for a shallow lake. It is also worth mentioning that in the LakeMIP project (Stepanenko et al. 2010), Lake Kossenblatter (2 m deep and $\sim 3 \text{ km}^2$ in size) in Germany, one of the lakes chosen for model intercomparisons, has a similar depth as Lake Taihu. Unlike this study, the results from LakeMIP show that the parameterization yields good estimation of T_s at Lake Kossenblatter. Similar conclusions are reached by Martynov et al. (2010) for Sparkling Lake, Wisconsin (depth 10.9 m, size 0.75 km^2). We note that T_s at both Lake Kossenblatter and the Sparkling Lake has diurnal variations noticeably smaller than that of Lake Taihu, suggesting stronger heat transfer between the surface and the deeper water in Lake Kossenblatter and Sparkling Lake. We postulate that the weak vertical mixing in Lake Taihu is related to the slow water movement (water residence time ~ 350 days) (An and Wang 2008) and small depth-to-size ratio of the lake. Lake Taihu probably has the largest fetch among the shallow lakes on earth. Because of its large surface area ($\sim 2500 \text{ km}^2$) and shallow depth (2.0 m), the drag force of the lake sediment layer may have been strong enough to prevent unresolved three-dimensional motions and to suppress wind-induced turbulence.

The adjusted k_e is in broad agreement with the eddy diffusivity determined in experimental studies. The simulated value varied mostly between 0.1 and $4 (\times 10^{-5} \text{ m}^2 \text{ s}^{-1})$ (Fig. 2c), with high values occurring at high wind conditions and during nocturnal overturning events. For comparison, field measurements of k_e at 19 shallow lakes (depth $< 30 \text{ m}$) fall in the range from 0.1×10^{-7} to $5 \times 10^{-5} \text{ m}^2 \text{ s}^{-1}$ (Benoit and Hemond 1996). These values are one to two orders of magnitude greater than the molecular diffusivity of heat in water. Similarly small diffusivity values have been simulated with a k – ϵ model for a shallow lake in Minnesota (Herb and Stefan 2005).

Concerns were expressed as to whether the small k_e was an artifact of the choice of T_s as the target variable for tuning. The reason for optimizing the model against T_s is that it is the surface temperature that drives the exchanges of sensible and latent heat with the air above. Indeed, the bulk heat flux formulations are all based on this temperature. Recognizing that CLM4 does not have a separate module for temperature of the interfacial surface layer (Liss 1973), we also tried an alternative approach by optimizing the model against the water temperature at a depth of 20 cm (case f in Fig. 3d). Forcing agreement of the modeled T_s with the observed temperature at this depth requires a scale factor of 0.08 for k_e . Thus, the overall conclusion—that a substantial

reduction of the eddy diffusivity is required to improve the model performance—is not adversely affected by the tuning process.

Based on Fig. 3c, there is room for improvement on temperature profile simulations. In comparison with the observation, the simulated temperature gradient in the top 1-m water column was much too strong on DOYs 235–237. This problem, along with the fact that the scale factor is dependent on the choice of the target temperature for optimization, reveals limitations of the Henderson-Sellers (1985) eddy diffusivity model for simulating fine-scale temperature profiles in shallow lakes. We suspect that other lake models that do not have an explicit parameterization of the interfacial layer physics may also experience similar difficulty. In this regard, the scale factor may be interpreted as an empirical adjustment for the practical purpose of predicting T_s and the surface heat fluxes.

Figure 3d shows the T_s simulation for the period from DOY 229 to 238 under different scenarios of k_e , roughness length, and light extinction parameter values. Among these scenarios, the CLM4-LISSS with default parameters (case b) yielded the smallest diurnal variation of T_s . As noted above, the reason for this is that the default k_e was too large for the lake, resulting in too strong vertical mixing. With k_e scaled down to 2% of its default values (case c), the diurnal variation of T_s matched closely with the observations, in terms of both amplitude and phase.

In case d, a step change of η from 5 to 1.4 m^{-1} occurred on DOY 232. This latter value is given by the CLM4-LISSS parameterization for a lake depth of 2 m. The results show the transient response of the lake temperature to changes in water quality. Improved water quality allowed more solar energy to be stored in the deeper water in daytime and the stored heat was released at night, reducing the diurnal range of T_s by about a small amount (0.2°C). The sensitivity analysis suggests that spatial variations in turbidity across the lake (Wang et al. 2011) are unlikely to generate measurable variations in the surface sensible and latent heat fluxes.

The difference between cases c and e indicates the effect of roughness parameterization on the T_s simulation. In case e, k_e was 2% of the default value, and the default, wind-dependent roughness lengths were used (Oleson et al. 2004). Over the period shown in Fig. 3, the default roughness length had mean values of 8.7×10^{-4} for momentum and 3.3×10^{-6} for heat and water vapor, which are larger than the values determined according to the field observation ($z_{0m} = 3.3 \times 10^{-4} \text{ m}$, $z_{0h} = 1.9 \times 10^{-6} \text{ m}$, $z_{0q} = 3.9 \times 10^{-8} \text{ m}$; case c). The model with the default roughness parameters produced good T_s prediction in the daytime but overestimated T_s at night; this

asymmetrical diurnal behavior could be the result of some unknown interactions of the surface–air exchange with the stability status of the water body. It was through the combination of reduced k_e and roughness that the model produced the correct diurnal T_s (case c).

To further rule out computational artifacts, we carried out one additional simulation by using the default surface roughness, the default eddy diffusivity, and the standard β value of 0.4 (Stepanenko et al. 2010). The variations in the modeled surface temperature time series were nearly identical to those of case b and were still too small compared to the observed values.

b. Seasonal variations

It is not surprising that both the default and tuned version of CLM4-LISSS captured the seasonal variations of T_s reasonably well (Fig. 4). Because of the lake's small thermal inertia and the lack of ice formation, T_s was tightly coupled with variations in air temperature, which were provided by the observations as a forcing variable of the model. However, throughout the year the predicted diurnal variation is lower than the observed value in the default case (Fig. 4, top). In contrast, the improvement of the calibrated version is evident at the diurnal time scale in all the seasons (Fig. 4, bottom).

Frontal passages significantly increase the fluxes of sensible heat and water vapor from lakes to the atmosphere (Blanken et al. 2011; Liu et al. 2011). The flux enhancement is caused by the large water-to-air gradients in temperature and humidity during frontal events. Two frontal events are shown in the insets to Fig. 4. The T_s predicted with the default k_e was delayed in reference to the observed time series in both events and did not reach the lowest observed temperature (insets to Fig. 4, top panel). These problems were largely overcome with the tuned version (insets to Fig. 4, bottom panel). The default model overestimated the latent heat flux by about 80 and 30 W m^{-2} during frontal events around DOY 240 and 300, respectively. Tuning reduced the model bias to less than 5 W m^{-2} . (The downward-facing longwave radiation sensor failed during DOY 246–250. The surface temperature measurement during this period was gap filled with a regression equation using the observed air temperature, resulting in artificially large diurnal amplitudes.)

The results shown in Fig. 4 were obtained with the snow/ice module turned off. If the snow module was left active in the simulation, both versions of the model had high T_s biases during the winter period from DOY 350, 2010 to DOY 35, 2011. The bias error was around 5 K for the default version and 3 K for the calibration version. The reason for this may lie in the parameterizations of snow and ice formation, which were triggered whenever

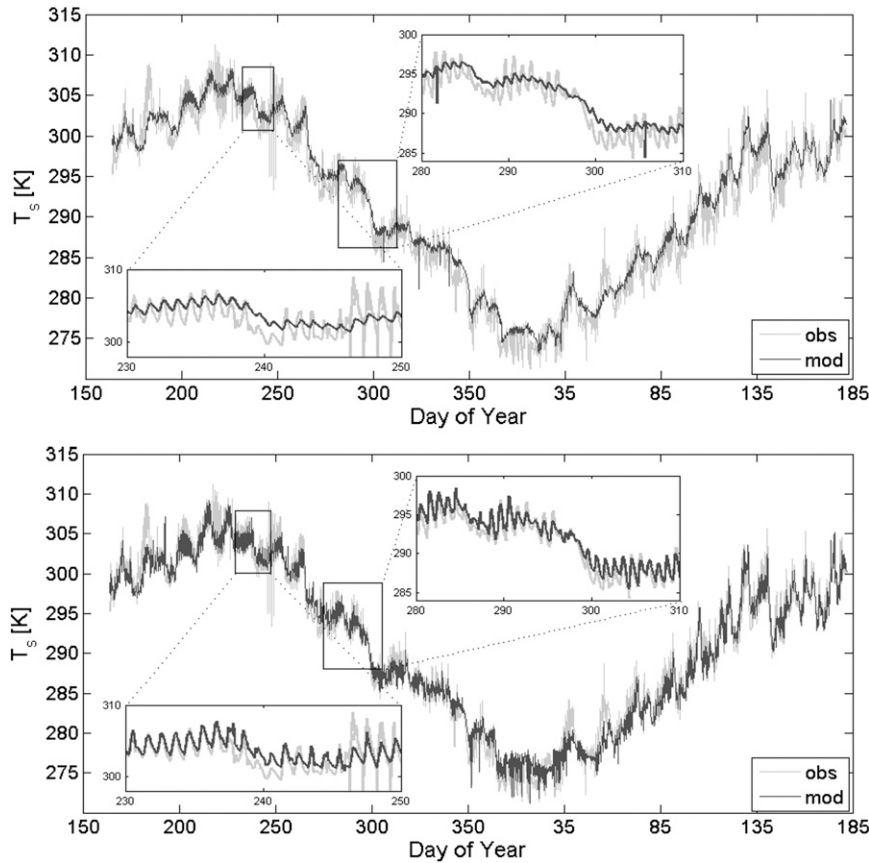


FIG. 4. Surface temperature T_s simulation from DOY 164 (2010) to DOY 183 (2011) based on (top) the default parameters of CLM-LISSS and (bottom) the calibrated version.

air temperature fell below the freezing point. During this time period, MLW recorded air temperature frequently below 0°C , but there was no ice formation and precipitation remained rain instead of snow.

c. Variations between sites

We now evaluate the performance of the calibrated CLM4-LISSS for a 40-day period in 2011 across the two measurement sites (Fig. 5), namely, the MLW site near the shoreline and the more offshore DPK site (Fig. 1). These two sites are about 30 km apart. They had similar water quality and water depth but markedly different wind speed. On average, wind speed at DPK was 84% greater than at MLW during this measurement period, so any differences between the sites can be used to gauge the effects of wind speed. The water surface temperature was nearly identical between the two sites, suggesting a low sensitivity to wind speed. If the model was driven by wind speeds at 50% of the observed values, the modeled surface temperature at DPK would increase by above 0.3 K, confirming the observed low wind sensitivity.

The predicted T_s agrees well with the observations at both sites. During a frontal event around DOY 144, the model reproduced very well the transient response of the lake surface temperature. The modeled T_s decreased from 302 to 290 K at DPK and MLW, nearly matching the observed values.

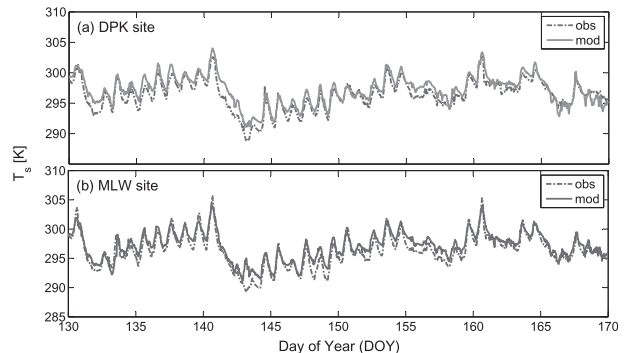


FIG. 5. Comparison between observed and model-predicted T_s in 2011 (based on the calibrated version of CLM-LISSS) at the (a) DPK site and (b) MLW site. The mean wind speed over this period was 3.8 and 2.1 m s^{-1} at DPK and MLW, respectively.

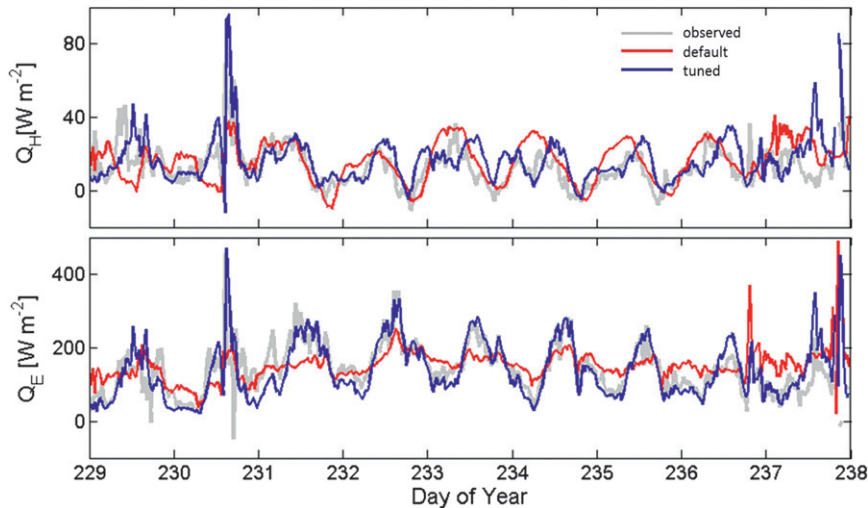


FIG. 6. Comparison between the observed and the model-predicted surface fluxes Q_H and Q_E (based on the default the calibrated version of CLM-LISSS) from DOY 229 to 238 (2010).

Across this large lake there exist spatial heterogeneities in water properties (e.g., turbidity) (Wang et al. 2011) and meteorological conditions (e.g., wind speed). An open question is whether a large lake like Lake Taihu can be represented with one grid cell in climate models or if these spatial heterogeneities can create large enough changes in the surface fluxes (Spence et al. 2011) to warrant the use of multiple grid cells. The lack of sensitivity of T_s to turbidity (Fig. 3d) and to wind (Fig. 5) suggests that spatial variations in sensible and latent heat fluxes may be small across Lake Taihu.

d. Surface heat fluxes

The half-hourly Q_E appeared more sensitive to the k_e and roughness parameterization than Q_H (Fig. 6). With the default parameters, the model reproduced reasonably well the magnitude of the diurnal variation in Q_H , but the predicted daily peak value was approximately 4 h in advance of the observed peak. The prediction of Q_E with default parameter values shows very small peak-to-peak diurnal variations. With the k_e adjustment, the phase mismatch in Q_H was largely erased, and the diurnal variations in Q_E were also predicted more correctly. For the period shown in Fig. 6, the R^2 value for the Q_E predictions was 0.85 with the k_e adjustment, higher than the R^2 value of 0.73 with the default model parameter values.

The multiday mean sensible and latent heat fluxes were less sensitive to the choice of parameterization scheme than the half-hourly values. The observed mean Q_H and Q_E were 19.3 and 123.7 W m^{-2} , respectively, over the period shown in Fig. 6. The mean values were 21.4 and 128.6 W m^{-2} for Q_H and Q_E , respectively,

according to the default model. These values change to 19.8 and 124.9 W m^{-2} if the calibrated model was used. Despite this lack of sensitivity in the mean fluxes to the model tuning, we suggest that correct prediction of both diurnal phases and hourly fluxes should improve applications such as calculation of the PBL growth and prediction of lake–land circulations.

The diurnal composite fluxes of radiation and energy reveal the dynamic adjustment of various energy transfer processes in response to solar radiation forcing (Fig. 7, top). Averaged over the year, roughly 30% of the net shortwave radiation was transmitted below the surface layer [term $(1 - \beta)K^*$]. Heat diffusion was directed downward (positive Q_g) between 0900 and 1500 local time and upward at other times. Averaged over the year, $(1 - \beta)K^*$ was balanced exactly by Q_g (see explanation below). The nighttime upward diffusion flux was quite large, approximately -110 W m^{-2} at midnight (the negative sign here indicates upward diffusion of heat). It was this flux that supplied energy for the positive (upward) nighttime latent heat ($\sim 25 \text{ W m}^{-2}$) and sensible heat flux ($\sim 10 \text{ W m}^{-2}$) and the net longwave radiation loss ($\sim 75 \text{ W m}^{-2}$). The diurnal course of the heat storage term [$Q_g + (1 - \beta)K^*$, Eq. (2)] of this shallow lake resembles the seasonal variation in the heat storage in deep lakes. Blanken et al. (2011) observed that heat is stored in the water in Lake Superior during the warm season, and the stored heat is diffused to the surface layer to fuel substantial evaporative and sensible heat fluxes in the cold season. Their cold season heat storage term is on the order of -300 W m^{-2} , or three times the nighttime storage flux in Lake Taihu. In other words, near deep lakes, modulation of the local climate via heat

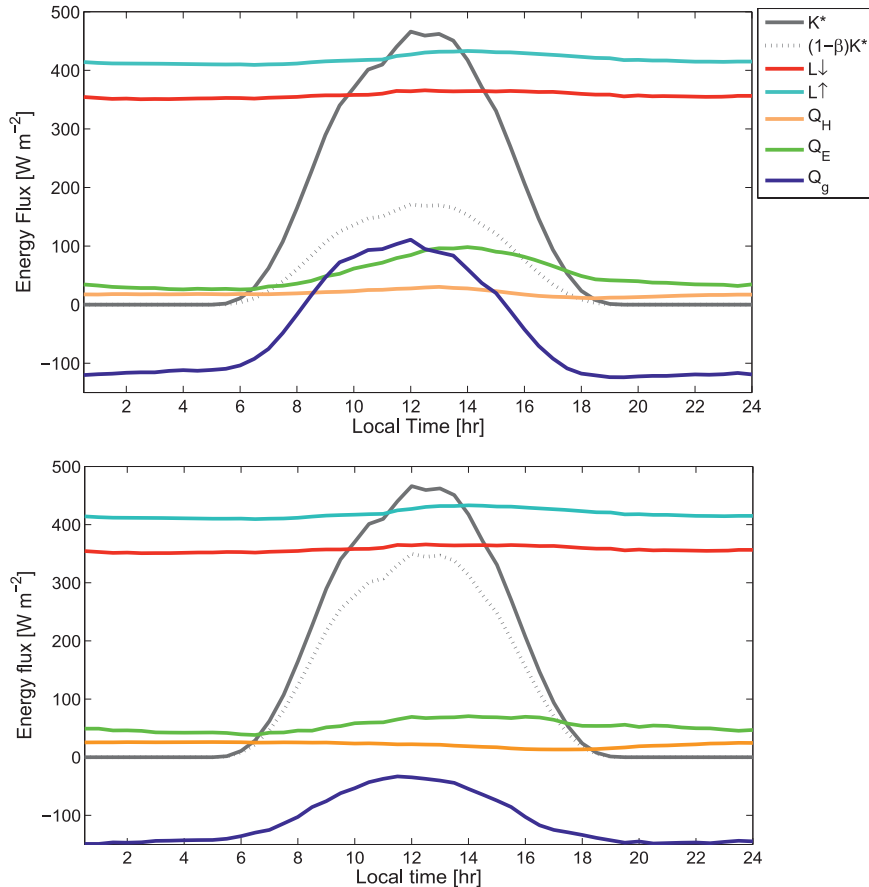


FIG. 7. Diurnal composite of radiation and energy balance components over one full annual cycle, DOY 183 (2010) to DOY 183 (2011): (top) tuned k_e and adjusted η ($=5.0 \text{ m}^{-1}$) and (bottom) tuned k_e and default η ($=1.4 \text{ m}^{-1}$).

storage occurs on the seasonal time scale, whereas at shallow lakes, the modulation occurs on the diurnal time scale.

Over the annual time scale, the calibrated version improved the estimation of half-hourly Q_H and Q_E (Fig. 8). Without the tuning, the model explained 81% and 83% of the observed variations in Q_H and Q_E , respectively. With tuning, the R^2 values increased to 87% and 89%, respectively. The improvement resulted mostly from a better phase match with the observed time variations in these fluxes (Fig. 6). The model performance compares favorably with the model results reported by Martynov et al. (2010) and Stepanenko et al. (2010) for deeper lakes. At the MLW site, fetch was greater than 3 km for ~50% of the time and greater than 300 m for ~70% of the time. Screening for longer fetch did not bring appreciable improvement to the modeled fluxes.

Averaged over the annual time scale, we expect that the lake system (water and its sediment) is neither a source nor a sink of energy. In other words, the downward

transmission of solar radiation in the water should be balanced by the upward heat diffusion, resulting in zero heat storage:

$$Q_g + (1 - \beta)K^* = 0. \tag{4}$$

Thus, the annual mean surface energy balance equation (2) reduces to

$$K^* + (L_{\downarrow} - L_{\uparrow}) = Q_H + Q_E. \tag{5}$$

The model simulations did show energy conservation as required by Eq. (5) (Table 1). The energy balance residual [terms on the right side minus terms on the left of Eq. (5)] was -1.1 W m^{-2} with both the default and the calibrated version. Tuning did not have an appreciable effect on the annual mean Q_H and Q_E (Table 1), consistent with the results shown in Fig. 6 for the warm season.

Changes in water quality, as measured with the light extinction coefficient η , had little effect on the annual

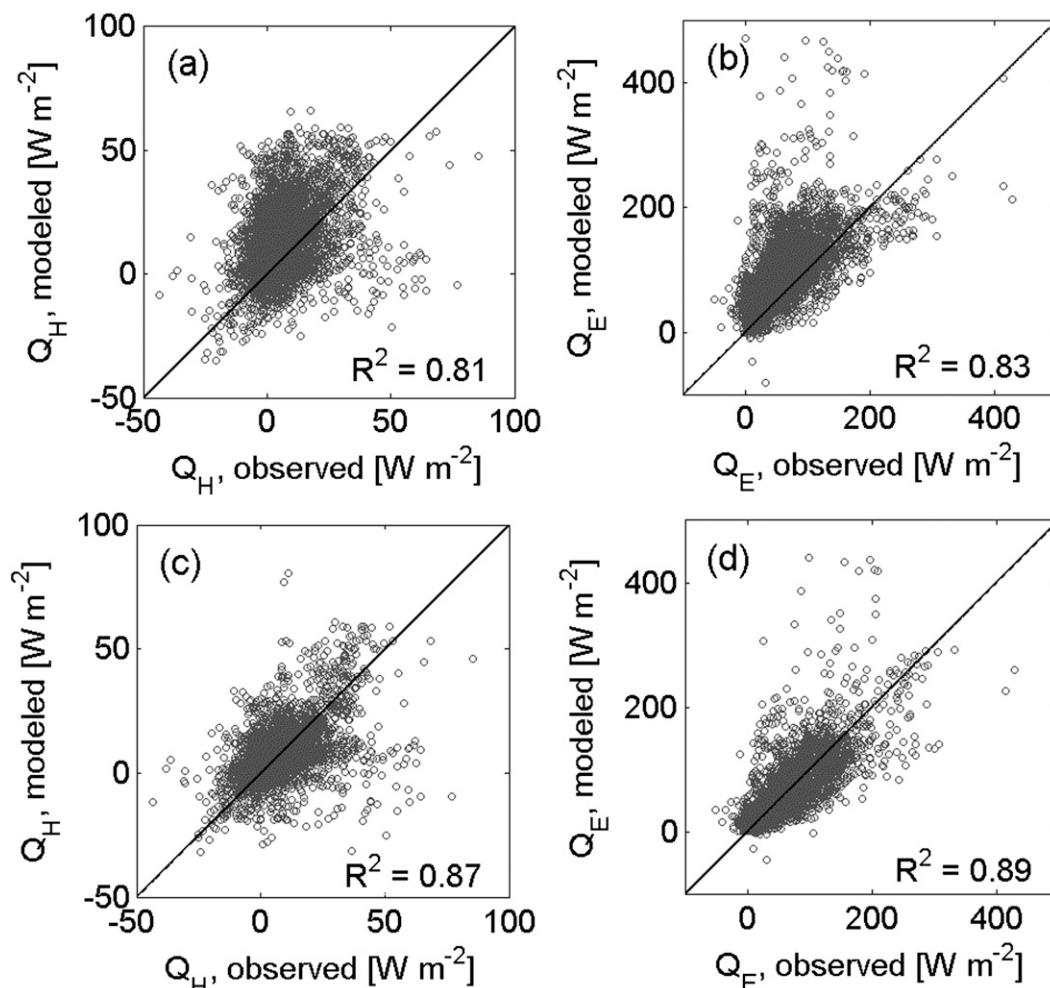


FIG. 8. Model-predicted surface fluxes Q_H and Q_E vs observations during gap-free periods from DOY 164 (2010) to DOY 183 (2011): (a),(b) default versions of CLM-LISSS and (c),(d) calibrated versions. The total number of half-hourly observations is 4169.

mean (Table 1) or the diurnal composite Q_H and Q_E (Fig. 7). However, in comparison to the polluted scenario ($\eta = 5.0 \text{ m}^{-1}$), in the clean scenario ($\eta = 1.4 \text{ m}^{-1}$) 44 W m^{-2} more solar energy was able to penetrate into the deep water and was stored there in daylight hours. The excess solar radiation transmission was compensated by the increase of a nearly identical amount in the upward diffusion heat flux (Table 1). According to the

diurnal composite results (Fig. 7), the nighttime diffusion flux was $\sim 70 \text{ W m}^{-2}$ more negative in the clean scenario than in the polluted scenario. Another notable difference is that the diffusion flux was negative (directed upward) throughout the day in the clean scenario, whereas it was positive between 0900 and 1500 in the polluted scenario. In other words, the interception of solar energy by the surface water layer warmed it enough

TABLE 1. Sensitivity analysis on annual (DOY 183, 2010 to DOY 183, 2011) mean radiation and energy balance components. In all three cases, K^* ($=131.3 \text{ W m}^{-2}$) and L_{\downarrow} ($=338.7 \text{ W m}^{-2}$) are forcing variables from the observations.

| Case | k_e | η (m^{-1}) | L_{\uparrow} (W m^{-2}) | Q_H (W m^{-2}) | Q_E (W m^{-2}) | Q_g (W m^{-2}) | T_s (K) | $(1 - \beta)K^*$ (W m^{-2}) |
|------|---------|-------------------------------|---|--------------------------------|--------------------------------|--------------------------------|--------------|---|
| A | Tuned | 5.0 | 398.9 | 22.4 | 49.8 | -55.9 | 289.5 | 55.6 |
| B | Default | 5.0 | 399.2 | 22.5 | 50.2 | -57.5 | 289.6 | 55.6 |
| C | Tuned | 1.4 | 398.6 | 22.2 | 48.1 | -99.5 | 289.4 | 99.9 |

to create a downward heat diffusion in the midday period in the polluted scenario but not in the clean scenario. The responses to water quality of solar radiation penetration and the diffusion heat flux, even though quite large, occurred in a compensating manner, which explains why Q_H and Q_E (Table 1, Fig. 7) and the surface temperature (Fig. 3) were insensitive to η .

4. Conclusions

The main purpose of this study is to calibrate the CLM4 lake model at the diurnal time scale using the direct flux observations at Lake Taihu. The most notable result is the amount of adjustment required of the eddy diffusivity k_e parameterization in order to improve the model performance at the diurnal time scale. The modeled lake surface temperature T_s is insensitive to turbidity and shows moderate sensitivity to a surface roughness parameterization. Because surface roughness was constrained by observations, we are left with k_e as the tunable model parameter. By reducing k_e to 2% of the value calculated with the parameterization of Henderson-Sellers (1985), CLM4-LISSS was able to reproduce the observed vertical thermal stratification and diurnal variations in T_s and to improve the T_s prediction during frontal disturbances. (Forcing agreement of the model with the observed temperature at the 20-cm depth requires a slightly larger scale factor of 0.08 for k_e .) We hypothesize that the drag force of the sediment layer in this large ($\sim 2500 \text{ km}^2$ size) and shallow (2-m depth) lake may have been strong enough to prevent unresolved vertical motions and to suppress wind-induced turbulence.

At this shallow lake, convective overturning occurred frequently at the time when the lake water switched from being stable during the day to becoming unstable shortly after sunset. Associated with the overturning was a one to two orders of magnitude increase in the eddy diffusivity. Even though it made little difference in the predicted seasonal and annual mean Q_H and Q_E , tuning of k_e brought improvement to the hourly fluxes. The calibrated model explained 87% and 89% of the observed variations in Q_H and Q_E , respectively.

Unlike deep lakes where heat storage in the water modulates the local climate at the seasonal time scale, near this shallow lake the modulation occurred at the diurnal time scale. A large fraction of the solar radiation energy was stored in the water during the daytime. The stored energy was then diffused up to the surface at night to sustain sensible and latent heat fluxes to the atmosphere. In the scenario of improved water quality, more solar radiation could be transmitted into the lower water layer, which was offset by a nearly identical enhancement

of upward heat diffusion, resulting in little change in the surface sensible and latent heat fluxes.

Two issues are worth further investigation. First, it remains an open question as to how much improvement the calibrated lake model can bring to predictions of lake–land breeze circulations and the PBL dynamics near the shoreline. Work is underway to fully couple the lake model with the operational Weather Research and Forecasting model for the lake catchment. Second, both the observations and the model simulations show that eddy mixing should vary strongly over the diurnal course in shallow lakes. Inclusion of this time-varying characteristic in parameterizations for the gas transfer coefficient (e.g., Cole and Caraco 1998) may improve calculations of the lake–air fluxes of trace gases.

Acknowledgments. This research was supported by the Ministry of Education of China (Grant PCSIRT), the Priority Academic Program Development of Jiangsu Higher Education Institutions (PARD), and the Natural Science Foundation of Jiangsu Province (Grant BK2011830).

REFERENCES

- An, S., and R. Wang, 2008: Human-induced drivers of the development of Lake Taihu. *Lectures on China's Environment*, X. Lee, Ed., Yale School of Forestry and Environmental Studies Publication Series, Vol. 20, Yale School of Forestry and Environmental Studies, 151–165.
- Battin, T. J., S. Luysaert, L. A. Kaplan, A. K. Aufdenkampe, A. Richter, and L. J. Tranvik, 2009: The boundless carbon cycle. *Nat. Geosci.*, **2**, 598–600.
- Benoit, G., and H. F. Hemond, 1996: Vertical eddy diffusion calculated by the flux gradient method: Significance of sediment-water heat exchange. *Limnol. Oceanogr.*, **41**, 157–168.
- Blanken, P. D., and Coauthors, 2000: Eddy covariance measurements of evaporation from Great Slave Lake, Northwest Territories, Canada. *Water Resour. Res.*, **36**, 1069–1077.
- , W. R. Rouse, and W. M. Schertzer, 2003: Enhancement of evaporation from a large northern lake by the entrainment of warm, dry air. *J. Hydrometeor.*, **4**, 680–693.
- , C. Spence, N. Hedstrom, and J. D. Lenters, 2011: Evaporation from Lake Superior: 1. Physical controls and processes. *J. Great Lakes Res.*, **37**, 707–716.
- Bonan, G. B., 1995: Sensitivity of a GCM simulation to inclusion of inland water surfaces. *J. Climate*, **8**, 2691–2704.
- Boyce, F. M., P. F. Hamblin, L. D. D. Harvey, W. M. Schertzer, and R. C. McCrimmon, 1993: Response of the thermal structure of Lake Ontario to deep cooling water withdrawals and to global warming. *J. Great Lakes Res.*, **19**, 603–616.
- Burchard, H., and H. Baumert, 1995: On the performance of a mixed-layer model based on the κ - ϵ turbulent closure. *J. Geophys. Res.*, **100**, 8523–8540.
- Cole, J. J., and N. F. Caraco, 1998: Atmospheric exchange of carbon dioxide in a low-wind oligotrophic lake measured by the addition of SF₆. *Limnol. Oceanogr.*, **43**, 647–656.
- , and Coauthors, 2007: Plumbing the global carbon cycle: Integrating inland waters into the terrestrial carbon budget. *Ecosystems*, **10**, 171–184.

- Desai, A. R., J. A. Austin, V. Bennington, and G. A. McKinley, 2009: Stronger winds over a large lake in response to weakening air-to-lake temperature gradient. *Nat. Geosci.*, **2**, 855–858.
- Downing, J. A., and Coauthors, 2006: The global abundance and size distribution of lakes, ponds, and impoundments. *Limnol. Oceanogr.*, **51**, 2388–2397.
- , and Coauthors, 2008: Sediment organic carbon burial in agriculturally eutrophic impoundments over the last century. *Global Biogeochem. Cycles*, **22**, GB1018, doi:10.1029/2006GB002854.
- Fang, X., and H. G. Stefan, 1998: Temperature variability in lake sediments. *Water Resour. Res.*, **34**, 717–729.
- Frew, N. M., and Coauthors, 2004: Air-sea gas transfer: Its dependence on wind stress, small-scale roughness, and surface films. *J. Geophys. Res.*, **109**, C08S17, doi:10.1029/2003JC002131.
- Goudsmit, G. H., H. Burchard, F. Peeters, and A. Wuest, 2002: Application of k- ϵ turbulence models to enclosed basins: The role of internal seiches. *J. Geophys. Res.*, **107**, 3230, doi:10.1029/2001JC000954.
- Heikinheimo, M., M. Kangas, T. Tourula, A. Venäläinen, and S. Tattari, 1999: Momentum and heat fluxes over lakes Tännaren and Råksjö determined by the bulk-aerodynamic and eddy-correlation methods. *Agric. For. Meteorol.*, **98–99**, 521–534.
- Henderson-Sellers, B., 1985: New formulation of eddy diffusion thermocline models. *Appl. Math. Modell.*, **9**, 441–446.
- Herb, W. R., and H. G. Stefan, 2005: Dynamics of vertical mixing in a shallow lake with submersed macrophytes. *Water Res. Res.*, **41**, W02023, doi:10.1029/2003WR002613.
- Hostetler, S. W., and P. J. Bartlein, 1990: Simulation of lake evaporation with application to modeling lake level variations of Harney-Malheur Lake, Oregon. *Water Resour. Res.*, **26**, 2603–2612.
- , G. T. Bates, and F. Giorgi, 1993: Interactive coupling of a lake thermal model with a regional climate model. *J. Geophys. Res.*, **98**, 5045–5057.
- , F. Giorgi, G. T. Bates, and P. J. Bartlein, 1994: Lake-atmosphere feedbacks associated with paleolakes Bonneville and Lahontan. *Science*, **263**, 665–668.
- Huang, C. C., Y. M. Li, C. F. Le, D. Y. Sun, L. Wu, L. Z. Wang, and X. Wang, 2009: Seasonal characteristics of the diffuse attenuation coefficient of Meiliang Bay waters and its primary contributors. *Acta Ecol. Sin.*, **29**, 3295–3306.
- Imberger, J., J. Patterson, B. Hebbert, and I. Loh, 1978: Dynamics of reservoir of medium size. *J. Hydraul. Div.*, **104**, 725–743.
- Krinner, G., 2003: Impact of lakes and wetlands on boreal climate. *J. Geophys. Res.*, **108**, 4520, doi:10.1029/2002JD002597.
- Laird, N. F., and D. A. R. Kristovich, 2002: Variations of sensible and latent heat fluxes from a Great Lakes buoy and associated synoptic weather patterns. *J. Hydrometeorol.*, **3**, 3–12.
- Lenters, J. D., T. K. Kratz, and C. J. Bowser, 2005: Effects of climate variability on lake evaporation: Results from a long-term energy budget study of Sparkling Lake, northern Wisconsin (USA). *J. Hydrol.*, **308**, 168–195.
- Liss, P. S., 1973: Processes of gas exchange across an air-water interface. *Deep-Sea Res.*, **20**, 221–238.
- Liu, H., Y. Zhang, S. Liu, H. Jiang, L. Sheng, and Q. L. Williams, 2009: Eddy covariance measurements of surface energy budget and evaporation in a cool season over southern open water in Mississippi. *J. Geophys. Res.*, **114**, D04110, doi:10.1029/2008JD010891.
- , P. D. Blanken, T. Weidinger, A. Nordbo, and T. Vesala, 2011: Variability in cold front activities modulating cool-season evaporation from a southern inland water in the USA. *Environ. Res. Lett.*, **6**, 024022, doi:10.1088/1748-9326/6/2/024022.
- Lofgren, B. M., 1997: Simulated effects of idealized Laurentian Great Lakes on regional and large-scale climate. *J. Climate*, **10**, 2847–2858.
- Long, Z., W. Perrie, J. Gyakum, D. Caya, and R. Laprise, 2007: Northern lake impacts on local seasonal climate. *J. Hydrometeorol.*, **8**, 881–896.
- MacKay, M. D., and Coauthors, 2009: Modeling lakes and reservoirs in the climate system. *Limnol. Oceanogr.*, **54**, 2315–2329.
- Martynov, A., L. Sushama, and R. Laprise, 2010: Simulation of temperate freezing lakes by one-dimensional lake models: Performance assessment for interactive coupling with regional climate models. *Boreal Environ. Res.*, **15**, 143–164.
- Mironov, D. V., 2008: Parameterization of lakes in numerical weather prediction: Description of a lake model. COSMO Tech. Rep. 11, Deutscher Wetterdienst, Offenbach am Main, Germany, 41 pp.
- Nordbo, A., S. Launiainen, I. Mammarella, M. Lepparanta, J. Huotari, A. Ojala, and T. Vesala, 2011: Long-term energy flux measurements and energy balance over a small boreal lake using eddy covariance technique. *J. Geophys. Res.*, **116**, D02119, doi:10.1029/2010JD014542.
- Oesch, D. C., J.-M. Jaquet, A. Hauser, and S. Wunderle, 2005: Lake surface water temperature retrieval using advanced very high resolution radiometer and Moderate Resolution Imaging Spectroradiometer data: Validation and feasibility study. *J. Geophys. Res.*, **110**, C12014, doi:10.1029/2004JC002857.
- Oleson, K. W., and Coauthors, 2004: Technical description of the Community Land Model (CLM). NCAR Tech. Note NCAR/TN 461+STR, 174 pp. [Available online at <http://nldr.library.ucar.edu/repository/assets/technotes/asset-000-000-000-537.pdf>.]
- Peeters, F., D. M. Livingstone, G. H. Goudsmit, R. Kipfer, and R. Forster, 2002: Modeling 50 years of historical temperature profiles in a large central European lake. *Limnol. Oceanogr.*, **47**, 186–197.
- Pegau, W. S., D. Gray, and J. R. V. Zaneveld, 1997: Absorption and attenuation of visible and near-infrared light in water: Dependence on temperature and salinity. *Appl. Opt.*, **36**, 6035–6046.
- Perroud, M., S. Goyette, A. Martynov, M. Beniston, and O. Anneville, 2009: Simulation of multiannual thermal profiles in deep Lake Geneva: A comparison of one-dimensional lake models. *Limnol. Oceanogr.*, **54**, 1574–1594.
- Rouse, W. R., P. D. Blanken, N. Bussières, C. J. Oswald, W. M. Schertzer, C. Spence, and A. E. Walker, 2008: Investigation of the thermal and energy balance regimes of Great Slave and Great Bear Lakes. *J. Hydrometeorol.*, **9**, 1318–1333.
- Samuelsson, P., and M. Tjernström, 2001: Mesoscale flow modification induced by land-lake surface temperature and roughness differences. *J. Geophys. Res.*, **106**, 12 419–12 435.
- , E. Kourzeneva, and D. Mironov, 2010: The impact of lakes on the European climate as simulated by a regional climate model. *Boreal Environ. Res.*, **15**, 113–129.
- Shen, J., H. Yuan, E. Liu, J. Wang, and Y. Wang, 2011: Spatial distribution and stratigraphic characteristics of surface sediments in Taihu Lake, China. *Chin. Sci. Bull.*, **56**, 179–187.
- Spence, C., P. D. Blanken, N. Hedstrom, V. Fortin, and H. Wilson, 2011: Evaporation from Lake Superior: 2. Spatial distribution and variability. *J. Great Lakes Res.*, **37**, 717–724.
- Stepanenko, V. M., and V. N. Lykosov, 2005: Numerical simulation of heat and moisture transport in the “lake-soil” system. *Russ. J. Meteor. Hydrol.*, **3**, 95–104.

- , S. Goyette, A. Martynov, M. Perroud, X. Fang, and D. Mironov, 2010: First steps of a lake model intercomparison project: LakeMIP. *Boreal Environ. Res.*, **15**, 191–202.
- Subin, Z. M., L. N. Murphy, F. Li, C. Bonfils, and W. J. Riley, 2012a: Boreal lakes moderate seasonal and diurnal temperature variation and perturb atmospheric circulation: Analyses in the Community Earth System Model 1 (CESM1). *Tellus*, **64A**, 15639, doi:10.3402/tellusa.v64i0.15639.
- , W. J. Riley, and D. V. Mironov, 2012b: An improved lake model for climate simulations: Model structure, evaluation, and sensitivity analyses in CESM1. *J. Adv. Model. Earth Syst.*, **4**, M02001, doi:10.1029/2011MS000072.
- Törnblom, K., H. Bergström, and C. Johansson, 2007: Thermally driven mesoscale flows—Simulations and measurements. *Boreal Environ. Res.*, **12**, 623–641.
- Tranvik, L. J., and Coauthors, 2009: Lakes and reservoirs as regulators of carbon cycling and climate. *Limnol. Oceanogr.*, **54**, 2298–2314.
- Vesala, T., J. Huotari, Ü. Rannik, T. Suni, S. Smolander, A. Sogachev, S. Launiainen, and A. Ojala, 2006: Eddy covariance measurements of carbon exchange and latent and sensible heat fluxes over a boreal lake for a full open-water period. *J. Geophys. Res.*, **111**, D11101, doi:10.1029/2005JD006365.
- Voros, M., V. Istvanovics, and T. Weidinger, 2010: Applicability of the FLake model to Lake Balaton. *Boreal Environ. Res.*, **15**, 245–254.
- Wang, M., W. Shi, and J. Tang, 2011: Water property monitoring and assessment for China's inland Lake Taihu from MODIS-Aqua measurements. *Remote Sens. Environ.*, **115**, 841–854.
- Wood, E. F., and Coauthors, 1998: The project for intercomparison of land-surface parameterization schemes (PILPS) phase 2(c) Red–Arkansas River basin experiment: 1. Experimental description and summary intercomparisons. *Global Planet. Change*, **19**, 115–135.
- Zeng, X., M. Shaikh, Y. Dai, R. E. Dickinson, and R. Myneni, 2002: Coupling of the Common Land Model to the NCAR Community Climate Model. *J. Climate*, **15**, 1832–1854.
- Zhao, L., J. Jin, S.-Y. Wang, and M. B. Ek, 2012: Integration of remote-sensing data with WRF to improve lake-effect precipitation simulations over the Great Lakes region. *J. Geophys. Res.*, **117**, D09102, doi:10.1029/2011JD016979.